

Electronic Supplementary Material (ESI) for Journal of Materials Chemistry A.  
This journal is © The Royal Society of Chemistry 2021

## Supporting Information

# Hollow Multishelled Heterostructures with Enhanced Performance for Laser Desorption/Ionization Mass Spectrometry based Metabolic Diagnosis

Congcong Pei,<sup>+a</sup> Rui Su,<sup>+b, c</sup> Songting Lu,<sup>+a</sup> Xiaonan Chen,<sup>a</sup> Yajie Ding,<sup>a</sup>  
Rongxin Li,<sup>a</sup> Weikang Shu,<sup>a</sup> Yu Zeng,<sup>a</sup> Yingying Lin,<sup>a</sup> Liang Xu,<sup>b</sup>  
Yuqiang Mi,\*<sup>b, c</sup> and Jingjing Wan\*<sup>a</sup>

<sup>a</sup>*School of Chemistry and Molecular Engineering, East China Normal University, Shanghai, 200241, P. R. China.*

<sup>b</sup>*Tianjin Second People's Hospital, Tianjin Medical University, Tianjin 300192, China.*

<sup>c</sup>*Tianjin Institute of Hepatology, Tianjin 300192, China*

\* Corresponding author:

Prof. Jingjing Wan (E-mail: jjwan@chem.ecnu.edu.cn.); Yuqiang Mi

(miyuqiang@tj.gov.cn)

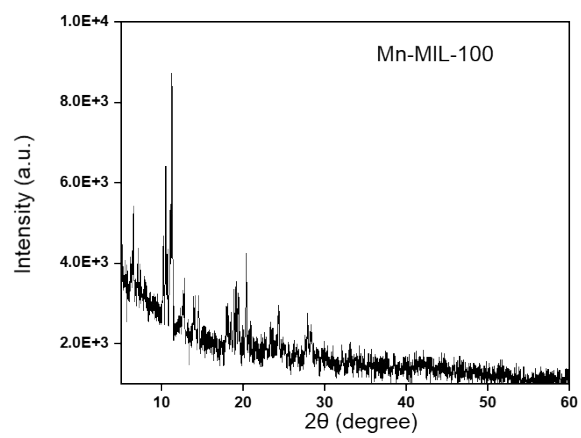


Fig. S1. XRD pattern of Mn-MIL-100.

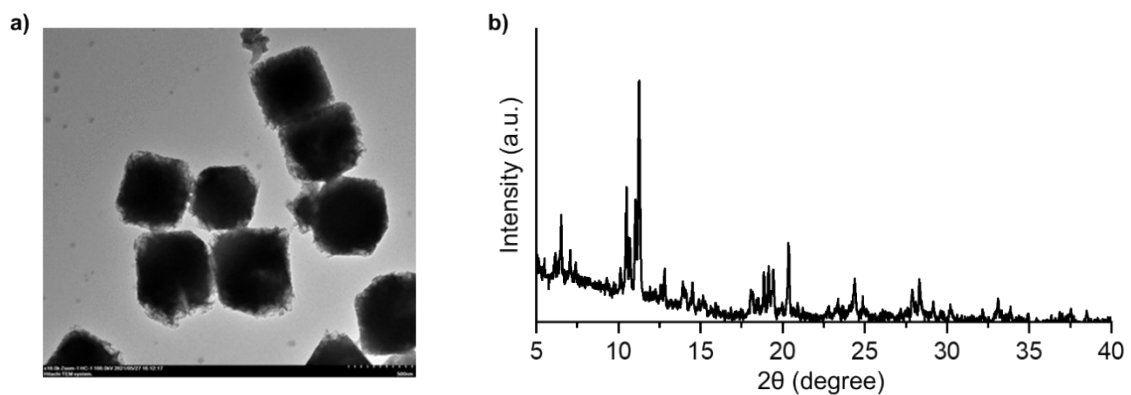


Fig. S2. a) TEM image and b) XRD pattern of slightly etched Mn-MIL-100.

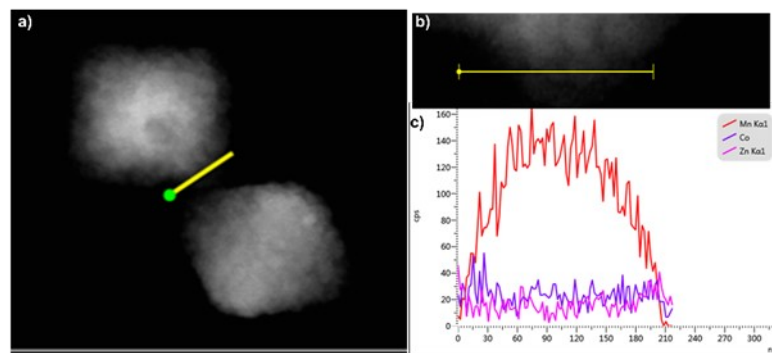


Fig. S3. STEM and line-scan (yellow line) EDX of Mn-MIL-100/ZIF.

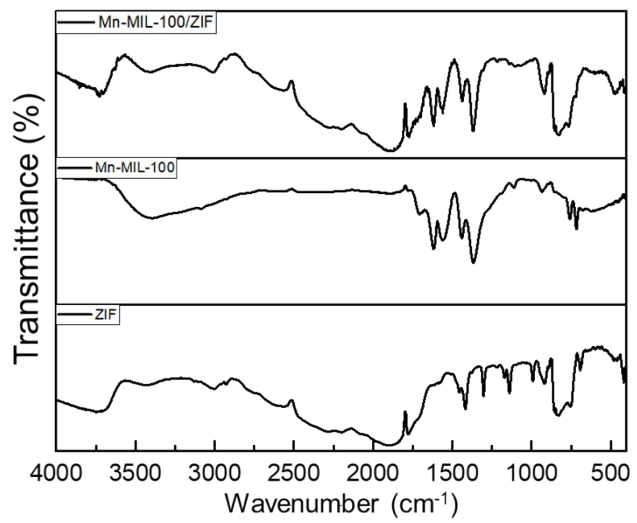


Fig. S4. FTIR spectra of ZIF, Mn-MIL-100, and Mn-MIL-100/ZIF.

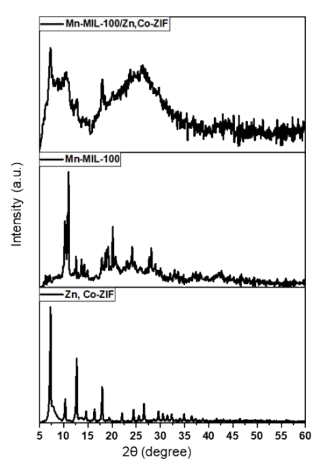


Fig. S5. XRD patterns of Zn, Co-ZIF, Mn-MIL-100, and Mn-MIL100/ZIF.

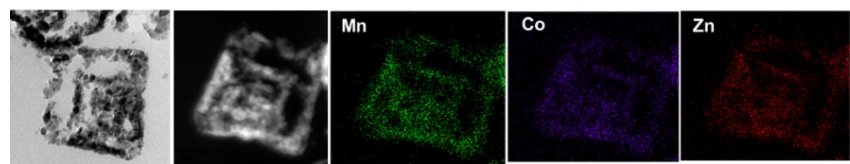


Fig. S6. TEM image, HADDF-STEM, and corresponding element mapping images of the TSH ZMO/CMO ultrathin slices.

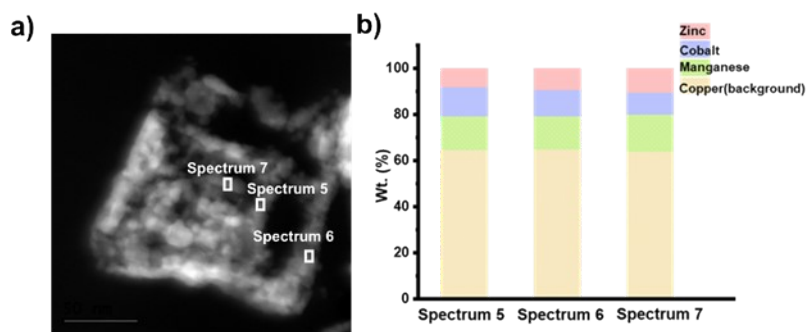


Fig. S7. a) HADDF-STEM image of ultrathin slices ZMO/CMO by ultramicrotomy; b) The wt% of elements in selected area elemental analysis of Fig. S7a.

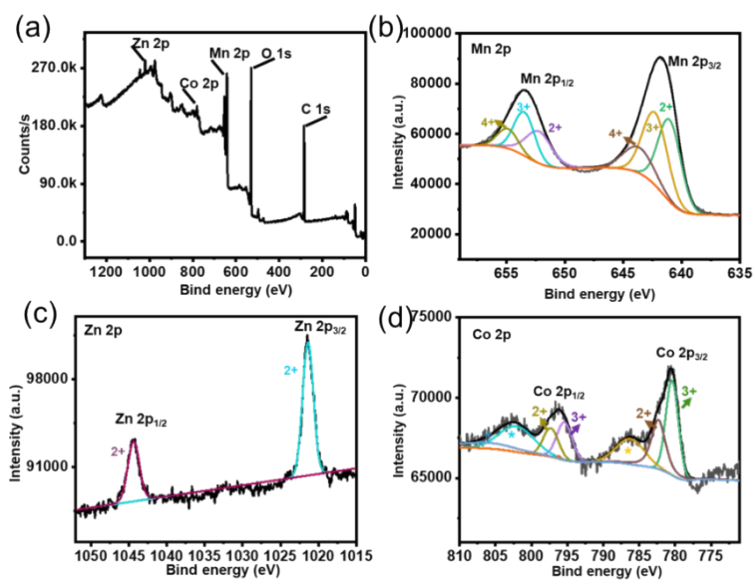


Fig. S8. XPS spectrum of TSH ZMO/CMO.

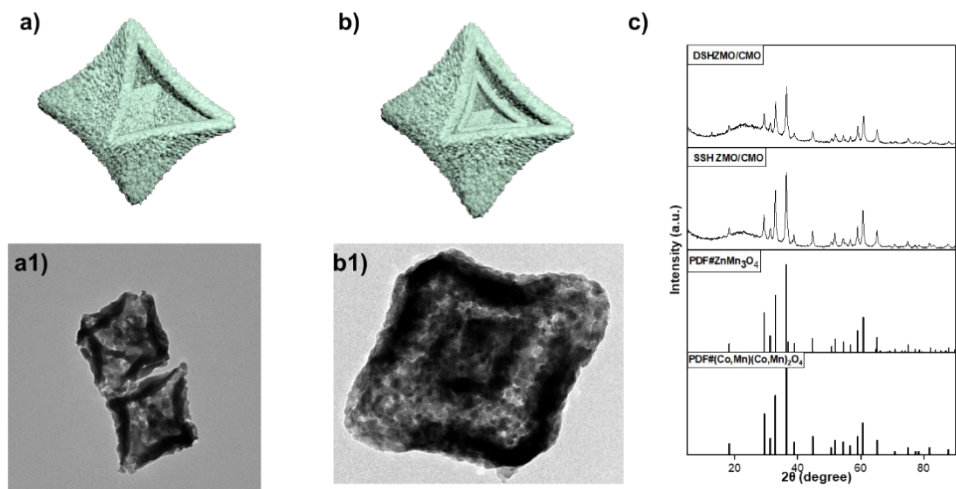


Fig. S9. TEM images of a) SSH ZMO/CMO and b) DSH ZMO/CMO; c) XRD spectrum of SSH ZMO/CMO and DSH ZMO/CMO.

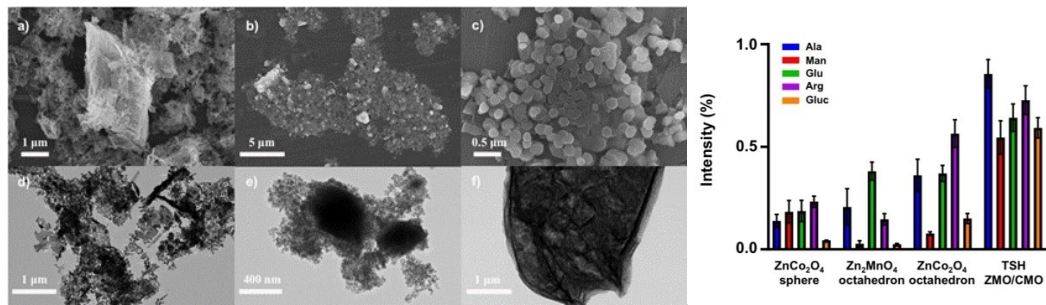


Fig. S10. (left) (a-c) SEM images of  $\text{ZnCo}_2\text{O}_4$  octahedron,  $\text{Zn}_2\text{MnO}_4$  octahedron, and  $\text{ZnCo}_2\text{O}_4$  sphere; (d-f) TEM images of  $\text{ZnCo}_2\text{O}_4$  octahedron,  $\text{Zn}_2\text{MnO}_4$  octahedron, and  $\text{ZnCo}_2\text{O}_4$  sphere. (right) Mean intensities of  $\text{Na}^+$  adducted peaks for Ala, Man, Glu, Arg and Gluc using  $\text{ZnCo}_2\text{O}_4$  sphere,  $\text{Zn}_2\text{MnO}_4$  octahedron,  $\text{ZnCo}_2\text{O}_4$  octahedron, and TSH ZMO/CMO as the matrices.

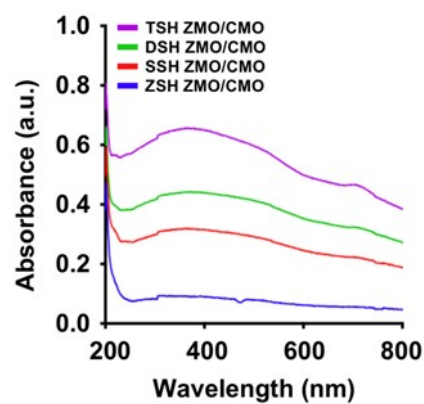


Fig. S11. The UV-vis absorption of ZSH, SSH, DSH, and TSH ZMO/CMO.

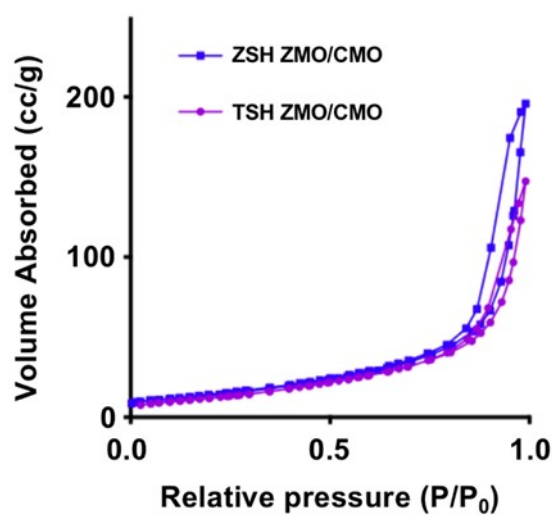


Fig. S12. Nitrogen adsorption isotherm of ZSH ZMO/CMO and TSH ZMO/CMO.

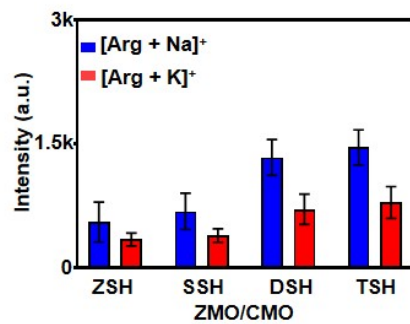


Fig. S13. Mean intensities of  $\text{Na}^+$  and  $\text{K}^+$  adducted peaks for 1  $\text{mg mL}^{-1}$  Arg using ZSH ZMO/CMO, SSH ZMO/CMO, DSH ZMO/CMO, and TSH ZMO/CMO as the matrices.

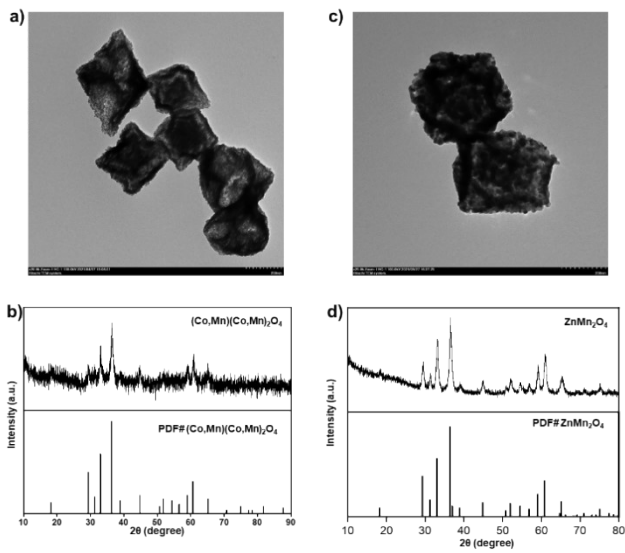


Fig. S14. a) TEM image and b) XRD pattern of  $(\text{Co},\text{Mn})(\text{Co},\text{Mn})_2\text{O}_4$ ; c) TEM image and d) XRD pattern of  $\text{ZnMn}_2\text{O}_4$ .

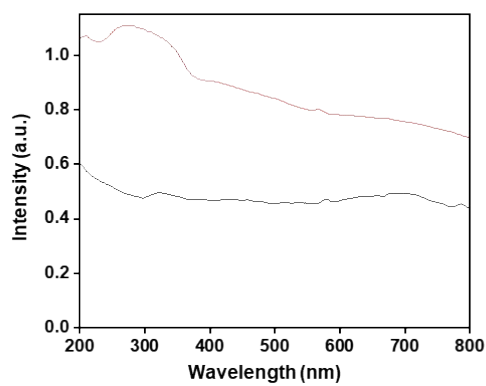


Fig. S15. The UV-vis DRS of TSH ZMO (grey line), TSH CMO (red line).

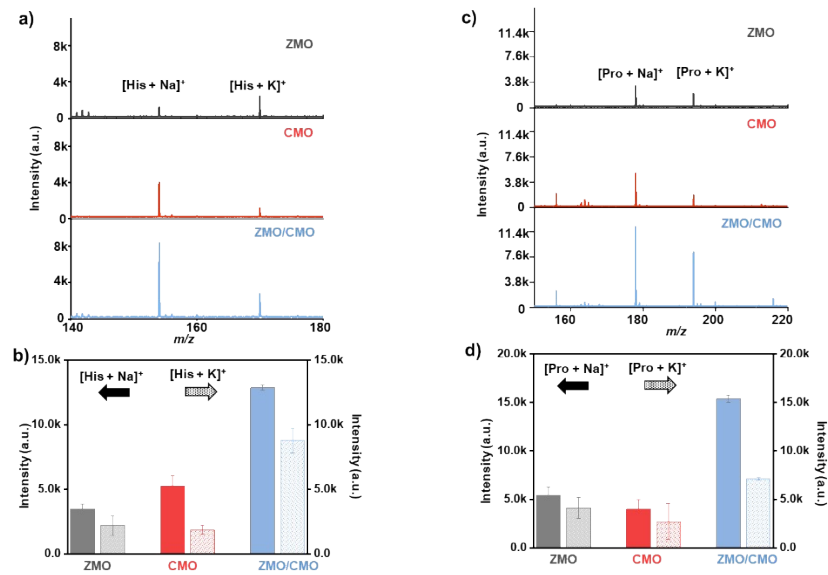


Fig. S16. Typical mass spectra of  $0.1 \text{ mg mL}^{-1}$  a) His and c) Pro using ZMO, CMO, and ZMO/CMO as the matrices; Mean intensities of  $\text{Na}^+$  and  $\text{K}^+$  adducted peaks for b)  $0.1 \text{ mg mL}^{-1}$  His, and d)  $0.1 \text{ mg mL}^{-1}$  Pro in 3 experiments using ZMO, CMO, and ZMO/CMO as the matrices.

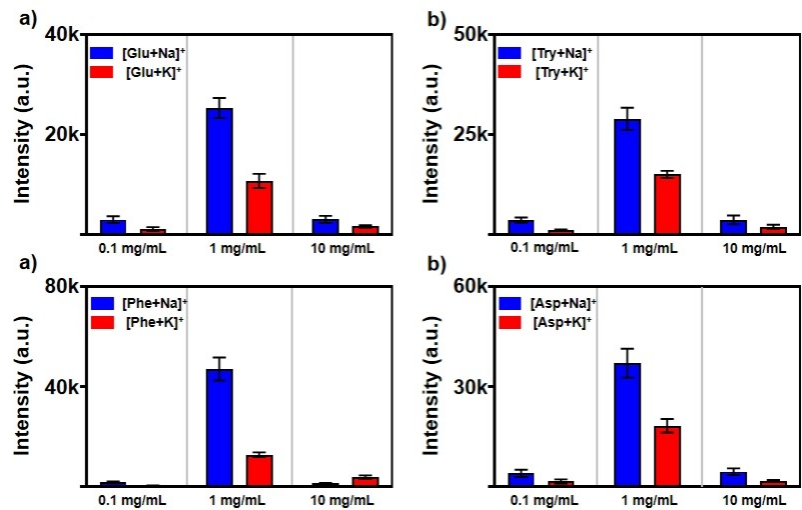


Fig. S17. Mean intensities of  $\text{Na}^+$  and  $\text{K}^+$  adducted peaks for Glu, Try, Phe, and Asp using  $0.1 \text{ mg mL}^{-1}$ ,  $1 \text{ mg mL}^{-1}$ ,  $10 \text{ mg mL}^{-1}$  TSH ZMO/CMO as the matrices.

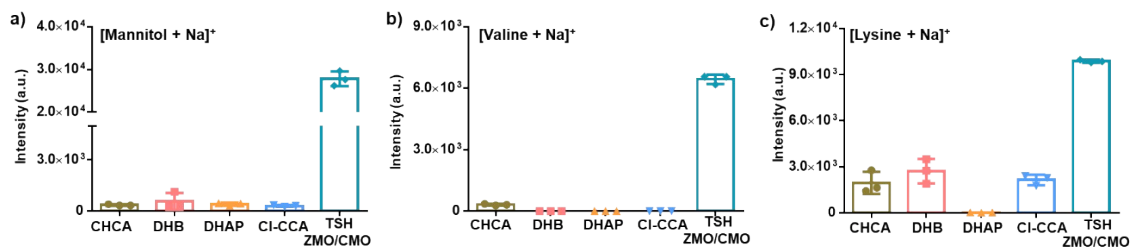


Fig. S18. The reproducibility of  $\text{Na}^+$  adducted peaks for a)  $0.1 \text{ mg mL}^{-1}$  Man, b)  $0.1 \text{ mg mL}^{-1}$  Val, and c)  $0.1 \text{ mg mL}^{-1}$  Lys in 3 experiments using CHCA, DHB, DHAP, Cl-CCA, and TSH MO/CMO as the matrices.



Fig. S19. The micrograph images of sample distribution with a) CHCA, b) DHB, c) DHAP, d) Cl-CCA, and e) TSH ZMO/CMO matrices.

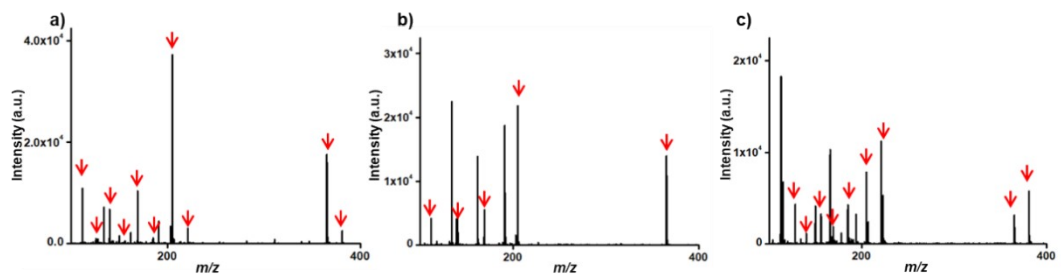


Fig. S20. Mass spectra of Ala, Lys, Val, Man, and Suc in a) 5.00 mg mL<sup>-1</sup> BSA and b) 0.50 M NaCl; c) 0.50 M KCl solutions using TSH ZMO/CMO as the matrix.

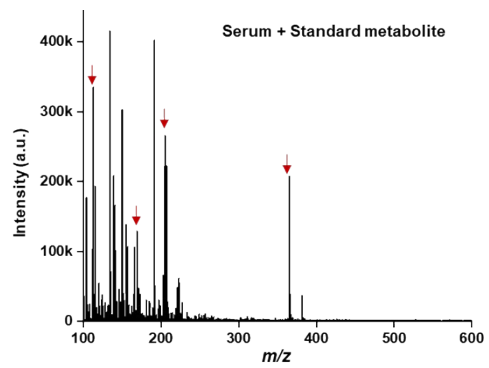


Fig. S21. The serum metabolic fingerprints of typical HCC serum and standard metabolites using TSH ZMO/CMO as the matrix.

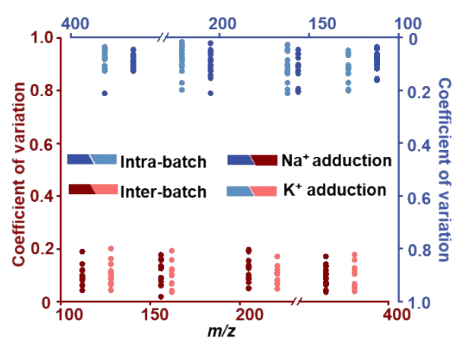


Fig. S22. CV distribution of intensities for the mixture of 4 analytes was loaded in serum.

Table. S1. Comparison of methods for multishelled materials.

Number	Cost (RMB)	Hazardous raw materials	Time	Morphology	Size	Component	Reference
1	0.79	/	24 h	triple-shelled octahedron	250 nm	ZnMn <sub>2</sub> O <sub>4</sub> /(Co, Mn) (Co, Mn) <sub>2</sub> O <sub>4</sub>	Our work
2	1.08	/	37 h	Single-shelled octahedron	6 $\mu$ m	ZnCo <sub>2</sub> O <sub>4</sub>	<sup>1</sup>
3	1.11	Nitric acid	24 h	Single-shelled octahedron	1.5 $\mu$ m	Zn <sub>2</sub> SnO <sub>4</sub>	<sup>2</sup>
4	10.48	/	32 h	triple-shelled sphere	1 $\mu$ m	ZnCo <sub>2</sub> O <sub>4</sub>	<sup>3</sup>
5	2.53	/	28.5 h	triple-shelled sphere	1 $\mu$ m	CuNiFe <sub>2</sub> O <sub>4</sub>	<sup>4</sup>
6	24.76	/	60.5 h	triple-shelled sphere	500 nm	Ni-Co-O	<sup>5</sup>
7	87.27	Sodium hydroxide	40.3 h	triple-shelled sphere	2 $\mu$ m	NiCo <sub>2</sub> O <sub>4</sub>	<sup>6</sup>
8	0.98	/	90 h	triple-shelled sphere	800 nm	Co <sub>2</sub> MnO <sub>4</sub>	<sup>7</sup>
9	67.60	/	51 h	triple-shelled sphere	1 $\mu$ m	TiO <sub>2</sub> /Fe <sub>2</sub> TiO <sub>5</sub>	<sup>8</sup>
10	0.37	/	29 h	triple-shelled sphere	700 nm	ZnMn <sub>2</sub> O <sub>4</sub>	<sup>9</sup>
11	673.85	Sodium hydroxide	21 h	double-shelled cube	1 $\mu$ m	Zn <sub>2</sub> SnO <sub>4</sub> -SnO <sub>2</sub>	<sup>10</sup>

Table. S2. The LOD and S/N ratio of the creatinine, Asp, and Glu.

	ZMO	CMO	SSH ZMO/CMO	DSH ZMO/CMO	TSH ZMO/CMO
Creatinine	0.005 mg/mL <b>S/N=18.7</b>	0.005mg/mL <b>S/N=20.4</b>	0.00005 mg/mL <b>S/N=9.3</b>	0.00001 mg/mL <b>S/N=6.2</b>	0.00001 mg/mL <b>S/N=7.2</b>
Aspartic acid	0.0005 mg/mL <b>S/N=8.3</b>	0.00001 mg/mL <b>S/N=12</b>	0.0001 mg/mL <b>S/N=9.4</b>	0.00001 mg/mL <b>S/N=4.1</b>	0.00001 mg/mL <b>S/N=6.2</b>
Glucose	0.01 mg/mL <b>S/N=16.4</b>	0.005 mg/mL <b>S/N=10.8</b>	0.0005 mg/mL <b>S/N=8.1</b>	0.00005 mg/mL <b>S/N=8.7</b>	0.00005 mg/mL <b>S/N=16.4</b>

Table. S3. Clinical characteristics of HCC patients and controls for training and test.

Characteristic	Training cohort		P value	Test cohort	
	HCC patient	control		HCC patient	control
Sex			0.911 <sup>a</sup>	/	/
Male	42	35	/	10	7
Female	30	26	/	6	2
Age (Median(ange))	61(41-81)	57(40-78)	0.414 <sup>b</sup>	/	/

<sup>a</sup>) P value was calculated by Chi-Square test; <sup>b</sup>) P value was calculated by t-test.

## Notes and references

1. J. Deng, X. Yu, X. Qin, B. Liu, Y.-B. He, B. Li and F. Kang, *Energy Storage Materials*, 2018, **11**, 184-190.
2. Z. Li, Y. Xiong, D. Bi, Q. Liu, C. Yang and J. Zhang, *Journal of Alloys and Compounds*, 2022, **901**, 163744.
3. D. Xue, F. Xue, X. Lin, F. Zong, J. Zhang and Q. Li, *Nanoscale*, 2019, **11**, 17478-17484.
4. M. Rajabzadeh, R. Khalifeh, H. Eshghi and M. Bakavoli, *Journal of Catalysis*, 2018, **360**, 261-269.
5. X. Li, L. Wang, J. Shi, N. Du and G. He, *ACS Applied Materials & Interfaces*, 2016, **8**, 17276-17283.
6. J. Wang, X. Yang, L. Xu, X. Liu, X. Li, G. Jia, S. Zhang and J. Du, *ACS Applied Nano Materials*, 2022, **5**, 9893-9900.
7. A. Indra, P. W. Menezes, C. Das, D. Schmeißer and M. Driess, *Chemical Communications*, 2017, **53**, 8641-8644.
8. M. Waqas, Y. Wei, D. Mao, J. Qi, Y. Yang, B. Wang and D. Wang, *Nano Research*, 2017, **10**, 3920-3928.
9. J. Xu, H. Zhang, R. Wang, P. Xu, Y. Tong, Q. Lu and F. Gao, *Langmuir*, 2018, **34**, 1242-1248.
10. L. Sun, X. Han, Z. Jiang, T. Ye, R. Li, X. Zhao and X. Han, *Nanoscale*, 2016, **8**, 12858-12862.